A portable multisensor system to assess cardiorespiratory interactions through photoplethysmography

Gabriele Volpes
Department of Engineering
University of Palermo
Palermo, Italy
gabriele.volpes@unipa.it

Laura Sparacino
Department of Engineering
University of Palermo
Palermo, Italy
laura.sparacino@unipa.it

Simone Valenti
Department of Engineering
University of Palermo
Palermo, Italy
simone.valenti@unipa.it

Antonino Parisi
Department of Engineering
University of Palermo
Palermo, Italy
antonino.parisi@unipa.it

Alessandro Busacca
Department of Engineering
University of Palermo
Palermo, Italy
alessandro.busacca@unipa.it

Luca Faes
Department of Engineering
University of Palermo
Palermo, Italy
luca.faes@unipa.it

Riccardo Pernice
Department of Engineering
University of Palermo
Palermo, Italy
riccardo.pernice@unipa.it

***Abstract*— Nowadays, the ever-growing interest to health and quality of life of individuals and the advancements in electronic devices technology are pushing the development of portable and wearable biomedical devices able to pursue a minimally invasive monitoring of physiological parameters in daily-life conditions. Such devices can now carry out a real-time assessment of the subjects' overall health status and possibly even detect ongoing diseases. In this context, we have designed and implemented a multisensor portable system able to perform synchronous real-time acquisitions of electrocardiographic (ECG), photoplethysmographic (PPG) and airflow breathing signals. We investigated cardiorespiratory interactions between heart period and respiratory time series, extracted from combined ECG and breathing signals (considered as the reference), or using the PPG signal only, through Granger Causality measures in time and frequency domain. The aim was to assess to what extent the non-invasive and cost-effective PPG technique can be employed alone to assess cardiorespiratory interactions, thus avoiding the simultaneous acquisitions of ECG or breathing signals with more bulky or uncomfortable devices. The analysis was carried out on 6 healthy young subjects, undergoing a two-phase protocol consisting in spontaneous and controlled breathing phases. Our findings show that linear interactions measures behave similarly if ECG or PPG are used for detecting the heart period and sampling the airflow respiratory signal, while the utilization of a respiratory signal extracted through filtering or as the envelope of the PPG waveform could lead to causality underestimates and must be further investigated.**

Keywords*— *Portable biomedical devices, electrocardiography (ECG); photoplethysmography (PPG); breathing signal; cardiorespiratory interactions; Granger causality.

I. INTRODUCTION

The widespread utilization of wearable devices is nowadays allowing to monitor in real-time and in a non-invasive manner several physiological parameters acquired from different body districts. Thanks to wearables, it is now possible to carry out a real-time assessment of subjects' health conditions and possibly even detect ongoing diseases, also opening new perspectives unthinkable until a few years ago. Recent works have in fact highlighted how the human organism can be considered as an integrated network in which nodes correspond to the organs continuously interacting with each other [1], [2]. Such interactions change over time in response to cognitive or homeostatic control mechanisms, to altered physiological states or to pathological conditions [1], [2]. Since the continuous dynamical interactions among organs are fundamental to maintain the homeostatic control, the role of wearable devices becomes pivotal to detect failures in such complex interaction mechanisms in a short time. Indeed, the real-time assessment of multiple physiological interactions may provide risk prediction indices useful to identify non-invasively an impairment of the physiological mechanisms that underlie possible pathological conditions.

The cardiac and respiratory systems provide a nice example of coupled biological oscillators [3] whose interactions have been studied during recent years, also playing a major role in some pathological conditions [3]–[6]. The well-known respiratory sinus arrhythmia (RSA), which is the direct pathway whereby neural commands originating in the respiratory centers of the brainstem act on the sinus node independently of blood pressure [7], has been studied for long time and can be detected during spontaneous as well as paced respiration [3], [5], [8]. The synchronous acquisition of cardiac and respiratory signals in non-clinical contexts would allow to assess the correct functioning of RSA, to detect changes in the cardiorespiratory coupling in real-life scenarios, such as during mental stress or apnoeic events during sleep [4], and to predict clinically risky situations thus avoiding severe complications. Specifically, the continuous monitoring of cardiac and respiratory parameters is essential in monitoring physiological control mechanisms and for an early detection of potentially pathological conditions driven by altered cardiorespiratory regulation. To extract clinically useful parameters from the cardiac and respiratory systems, a cost-efficient, low invasive, and easy-to-use technique is photoplethysmography (PPG); this technique allows to assess the blood volume changes through the variation of the light transmitted or reflected by the blood, and can be exploited in place of the well-known and most commonly used electrocardiographic (ECG) approach [9], [10].

In this work, we carry out a synchronous acquisition of cardiorespiratory signals (ECG, PPG and respiration) using a low-invasive multisensor acquisition system [10], [11]. Starting from the time series extracted from the signals, the strength of the causal interactions directed from the respiratory process to the heart period (HP) is assessed

through Granger Causality measures [12], [13]. The aim is to prove whether and to what extent the non-invasive and cost-effective PPG technique can be used alone to assess cardiorespiratory interactions without acquiring the ECG or breathing signals.

II. Materials and Methods

A. Measurement equipment and protocol

The portable system used in this study for acquiring the signals (shown in Fig. 1) consists of three key components: (i) a high-performance STM32-F401RE (by STMicroeletronics) ARM Cortex-M4 Reduced Instruction Set Computer (RISC) architecture microcontroller with a clock frequency of 84 MHz; (ii) a 24-bit resolution and low-noise analog-to-digital converter (ADS1298), supporting 8 channels specially designed for biosignal measurements; (iii) a Bluetooth module (SPBT3.0DP2) with 1.5Mbps high speed UART transmission. PPG signals were acquired using an appositely developed probe realized consisting of an infrared light source at 850 nm and a silicon photomultiplier (SiPM), which has a higher intrinsic gain than a conventional photodiode [14]. Standard peripheral clamp electrodes were used for acquiring the ECG signal. Finally, the breathing signal was recorded using a 10 kΩ negative thermistor (NTC) capable of detecting a voltage signal related to airflow that increases during the exhalation phase and decreases during the inhalation phase.

Three different signals were synchronously acquired, i.e. a two-lead electrocardiogram (ECG), the PPG signal and the respiratory signal. The four ECG electrodes were positioned according to the Einthoven's triangle on the wrists and legs [15]; the PPG probe was positioned on the left wrist; the breath probe was placed on the nose. All signals were sampled with 500 Hz sampling frequency and 24-bit resolution. An appositely developed GUI was used to show the acquired signals in real time and to send the recorded data wirelessly via Bluetooth to a personal computer, in order to save them for the subsequent offline analyses (we refer to [10], [11] for further information).

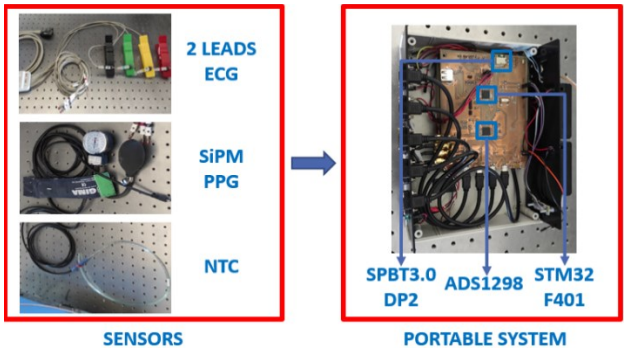

Fig. 1. Overview of our portable biomedical system.

Measurements were carried out on 6 healthy subjects (3 males and 3 females; 24.3 ± 1.9 years) monitored in a sitting position and undergoing a two-phase protocol aimed at assessing cardiorespiratory interactions during spontaneous (SB) and controlled breathing (CB, breathing rate: 20 breaths/min, i.e. 0.33 Hz). In order to ensure a correct execution of the paced breathing, the subjects were instructed to follow an appositely developed visual metronome application showing different colors according to the current breathing phase, i.e. inhalation/expiration (we refer the reader to [10] for further information).

B. Data preprocessing and time series analysis

The analyses were carried out using MATLAB 2019b software (The Mathworks, Inc, Natick, MA, USA). The acquired ECG, PPG and breathing (RESP) signals were first filtered using a zero-phase fourth-order Butterworth bandpass filter (ECG: [0.1-20 Hz], PPG and RESP: [0.1-15 Hz]). Starting from the ECG signals, the R peaks were detected using a modified version of the Pan-Tompkins algorithm [16] in order to extract the R-R interval (RRI) time series. With regard to PPG signals, a threshold-based peak detection algorithm was employed to locate the waveform minima of the acquired signal which have been then used for pulse-pulse interval (PPI) time series.

We also performed the reconstruction of the respiratory signal starting from the PPG signals, using both a filtering-based approach and Empirical Mode Decomposition (EMD) [17]. For the first approach, a bandpass filter was applied accounting for a range of respiratory frequencies determined in accordance with the knowledge that respiration variability usually falls within the HF band (0.15-0.4 Hz) [18], [19]; in two of the six subjects the range was adapted to take into account the respiratory peak falling out of the HF band (we chose (0.08-0.33 Hz) and (0.25-0.5 Hz) to detect peaks at ~0.1 Hz and ~0.45 Hz, respectively). The second method has been already widely used for extracting breathing rate from PPG signals (see e.g. [17], [20]). We have applied a simplified version of the EMD algorithm presented in [17], herein summarized:

(i) Find the local maxima (M_i) and the local minima (m_i) of the PPG signal ($x(t)$);

(ii) Interpolate the maxima and minima using the same number of points of the PPG, so as to generate the upper $M(t)$ and lower $m(t)$ envelopes, respectively (the MATLAB cubic spline interpolation algorithm was employed);

(iii) Compute the average envelope as $e(t) = \frac{M(t)+m(t)}{2}$;

(iv) Subtract the average envelope to the PPG signal, $x(t) := x(t) - e(t)$.

(v) The steps (i)-(iv) should be repeated until the new $x(t)$ does not vary from the $x(t)$ at the previous iteration. In our approach the EMD is stopped at the first loop, and the reconstructed breathing signal is selected as the average envelope [17].

Using the above approaches, four different respiration time series were extracted and used to compute cardiorespiratory interaction measures:

(i) R_RRI: series extracted as the values of the respiration signal sampled at the times of ECG R peaks;

(ii) R_PPI: series extracted as the values of the respiration signal sampled at the times of PPG peak minima;

(iii) R_PPG_filter: series extracted as the values of the respiration signal reconstructed through the filtering approach sampled at the times of PPG peak minima;

(iv) R_PPG_EMD: series extracted as the values of the respiration signal reconstructed through the EMD technique sampled at the times of PPG peak minima.

For all the time series (RRI, PPI and (i)-(iv) respiration series), 300-point stationary windows were extracted.

C. Cardiorespiratory interactions

This section reports the linear parametric computation of cardiorespiratory interactions. The analysis was performed considering both lagged and instantaneous (i.e., not delayed) effects from respiration (driver process, labelled as R) to the heart period (target process, labelled as H), as the common adopted measurement convention assumes that $R(n)$, sampled at the onset of the n^{th} RRI, could have a role in determining $H(n)$ variability [21]. The time series were first pre-processed using a high-pass autoregressive (AR) filter with cut-off frequency of 0.0156 times the sampling rate f_s, the latter computed for each subject assuming the series as uniformly sampled with sampling period equal to the mean heart period ⟨HP⟩. Each pair of stationary zero-mean H and R series forming the bivariate process $\boldsymbol{Y}(n)$ was then fitted by the extended AR model including zero-lag effects [22]:

$$\boldsymbol{Y}(n) = \sum_{k=0}^{p} \boldsymbol{B}(k)\boldsymbol{Y}(n-k) + U(n) \qquad (1)$$

where p is the model order and $\boldsymbol{Y}(n) = [Y_1(n)\ Y_2(n)\ ]^T$, with $Y_1 = H$ and $Y_2 = R$. The 2x2 coefficient matrix $\boldsymbol{B}(k)$ relates the present with the past of the processes assessed at lag k, the latter taking the value 0 as well to bring instantaneous effects from $Y_2(n)$ to $Y_1(n)$ into the model in the form of the coefficient $b_{12}(0)$ of the matrix $\boldsymbol{B}(0)$. The vector $\boldsymbol{U}(n) = [U_1(n)\ U_2(n)]^T$ contains zero-mean uncorrelated white noises, with diagonal covariance matrix $\boldsymbol{\Sigma} = E[\boldsymbol{U}(n)\boldsymbol{U}^T(n)] = diag\{\sigma_{ii}^2\}$, $i = 1,2$. While the full AR model in Eq. (1) provides a global representation of the bivariate process, to describe the individual dynamics of the target process Y_1, a reduced AR model involving only that process was formulated as:

$$Y_1(n) = \sum_{k=1}^{\infty} \tilde{a}_1(k)Y_1(n-k) + \tilde{U}_1(n), \qquad (2)$$

where the coefficients $\tilde{a}_1(k)$ weight the past samples of the process $Y_1(n)$, and the innovation process $\tilde{U}_1(n)$ has variance $\tilde{\sigma}_{11}^2$. Note that to capture the full dynamical behavior of $Y_1(n)$ the order of the restricted AR process is infinite even when the original bivariate model has a finite order p [23]. Identification of the full (1) and restricted (2) models was performed via the vector least-squares approach, setting the model order p according to the multivariate version of the Akaike Information Criterion (AIC) for each subject (with maximum scanned model order equal to 8) [24]. The linear parametric formulation allows to compute the logarithmic measure of Granger Causality [12], [13] by comparing the variance of the residuals resulting from the two regressions:

$$F_{j\to i} = ln\left(\frac{\tilde{\sigma}_{ii}^2}{\sigma_{ii}^2}\right). \qquad (3)$$

Moreover, from the full AR representation of the bivariate process (1), it is possible to represent the model coefficients in the Z domain through the Z-transform of Eq. (1), thus yielding $\boldsymbol{Y}(z) = \boldsymbol{H}(z)\boldsymbol{U}(z)$, where the 2x2 transfer matrix is computed as $\boldsymbol{H}(z) = [\boldsymbol{I} - \sum_{k=1}^{p} \boldsymbol{A}(k)z^{-k}]^{-1}$, being $\boldsymbol{I}$ the 2x2 identity matrix. Computing $\boldsymbol{H}(z)$ on the unit circle in the complex plane, it is possible to derive the spectral density matrix of the bivariate process as $\boldsymbol{S}(\bar{f}) = \boldsymbol{H}(\bar{f})\boldsymbol{\Sigma}\boldsymbol{H}^*(\bar{f})$, where $\bar{f} \in [-0.5,0.5]$ is the normalized angular frequency $\bar{f} = f/f_s$, and * stands for the Hermitian transpose. This matrix contains the power spectral densities (PSDs) of the individual processes on the diagonal, and the cross PSDs between the two processes out of the diagonal. The PSD of the respiratory process in the HF band was computed as the integral of the auto-spectrum within the HF band, normalized with respect to the total power (i.e., the integral of the spectrum alongside the whole frequency axis) and labelled as $P_2(HF)$. Moreover, a frequency-specific measure of Granger causality from Y_j to Y_i was computed as [13]:

$$f_{j\to i}(\bar{f}) = ln\left(\frac{S_{ii}(\bar{f})}{\sigma_{ii}^2|H_{ii}(\bar{f})|^2}\right), \qquad (4)$$

and interpreted as a measure of coupling strength, being 0 in the absence of directed coupling from Y_j to Y_i at the frequency $\bar{f}$, and increasing to infinite in the presence of full coupling. The integration of Eq. (4) alongside the whole frequency axis, with the Nyquist frequency in each spectral representation taken as $f_s/2 = 1/(2\langle HP\rangle)$, provides the correspondent time domain measure given in Eq. (3), i.e. we have $F_{j\to i} = 2\int_0^{1/2} f_{j\to i}(\bar{f})d\bar{f}$ [25]. To study the causal effect from respiration to the heart period, we computed Eq. (4) from $Y_2(n)$ to $Y_1(n)$, and labelled it as $f_{2\to 1}(\bar{f})$, then integrated this spectral distribution alongside the whole frequency axis to obtain $F_{2\to 1}$, and within the HF band of the spectrum, thus obtaining the value $f_{2\to 1}(HF)$. The width of the HF band was determined individually for each subject by first locating the respiratory peak and then selecting the band with a width of ±0.06 Hz around such peak.

III. Results and Discussion

Figure 2 shows an example of ECG, PPG and breathing signals synchronously acquired using our portable system. Figure 3(a) depicts the extraction of the breathing signal (in black) as the average of maxima and minima envelopes of PPG signal through the EMD algorithm. Figures 3(b) and (c) depict the breathing signals obtained after EMD and using the HF-band filtering procedure, respectively, compared to the reference airflow breathing signal acquired using the NTC (Fig. 3(d)). Figure 4 shows an example of the four respiration time series extracted according to the approaches described in Section II.B, from both the acquired and reconstructed respiration signal. In detail, we considered as the reference the series obtained as the points in the acquired breathing signal corresponding to the timing of ECG R peaks (R_RRI), shown in Fig. 4(a)), while the corresponding R_PPI series is depicted in Fig. 4(b). The two respiration series reconstructed only using PPG through filtering and through EMD are shown in Fig. 4(c) and Fig. 4(d), respectively. It is possible to note that the respiration series obtained sampling the airflow signal (Fig. 4a,b) are very similar to each other, and differ from those obtained sampling the PPG-derived respiration signal (Fig. 4c,d). Figure 5 shows the subject-specific results of time domain and spectral analysis. The computed measures were the normalized PSD of the respiratory process (Fig. 5(a)), the time domain Granger causality (Fig. 5(b)) and the spectral Granger causality integrated within the HF band of the spectrum (Fig. 5(c)), in both phases of the protocol (panels above: SB; panels below: CB). We have analysed the following combinations of respiratory and heart period time series: (i) heart period: RRI time series extracted from ECG; respiratory time series: R_RRI; (ii) heart period: PPI time series extracted from PPG; respiratory time series: R_PPI; (iii) heart period: PPI time series extracted from PPG; respiratory

time series: R_PPG_filt; (iv) heart period: PPI time series extracted from PPG; respiratory time series: R_PPG_EMD.

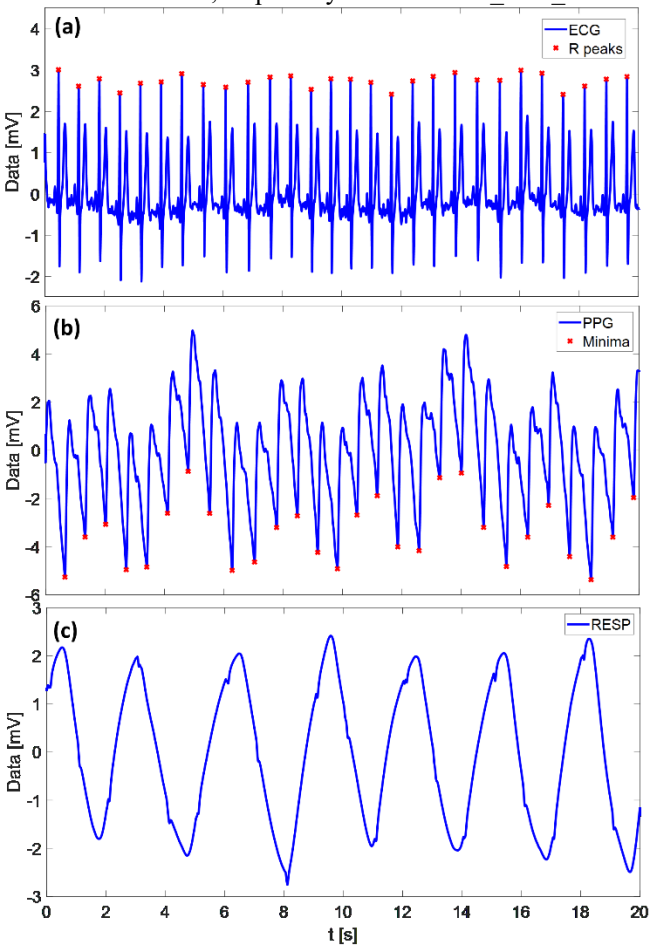

Fig. 2. Examples of (a) ECG, (b) PPG and (c) airflow breathing signals synchronously acquired using our portable system. In (a) the ECG R peaks are indicated with red cross markers. In (b) the minima peaks are indicated with red cross markers.

Our results are dependent on the very small dataset used. Two subjects presented spontaneous breathing rates higher or lower than usual (respectively, ~0.45 Hz and ~0.1 Hz), falling out of the frequency band commonly referred to as respiratory band [0.15-0.4 Hz]. Surprisingly, it has been previously found that, in many healthy subjects, breathing frequency slows down to the LF band and entrainment of the cardiovascular rhythm around 0.1 Hz often occurs [26]. In our study, slow breathing was found in one of the six subjects who performed the experimental protocol. This put a constraint in the selection of the HF band for the computation of spectral measures, as we have chosen subject-specific HF ranges to take into account possible outliers. However, this approach may cause to fail detecting the whole power in HF band. Indeed, we noticed that the bandwidth around the peak is larger when reconstructing the respiration signals from PPG (i.e. R_PPI_filter and R_PPI_EMD) for both experimental conditions (SB, CB), probably due to "spurious" spectral content related to autonomic system activity not present in the "true" respiration-only signal. This may be the reason of the unexpected sudden decrease of respiratory PSD in HF when extracting RESP from PPG, both with filtering and EMD approaches, mostly visible in one of the subjects (e.g. orange point in Fig. 5(a)) but generally occurring for all of them in both experimental conditions.

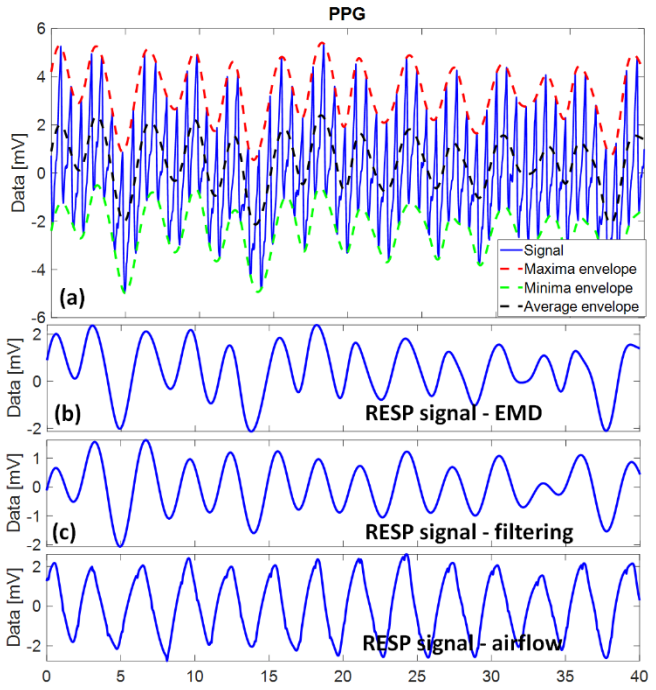

Fig. 3. Reconstruction of respiration signals from the PPG waveform: (a) Illustration of extraction procedure through the EMD algorithm: starting from the PPG signal (blue line), the maxima (red dotted line) and minima (green dotted line) envelopes are obtained, and their average (black dotted line) represents the reconstructed breathing signal, shown in (b). (c) Reconstructed respiration signal through band-pass filtering [cut off frequencies: 0.15-0.4 Hz]. (d) "True" airflow breathing signal acquired through NTC.

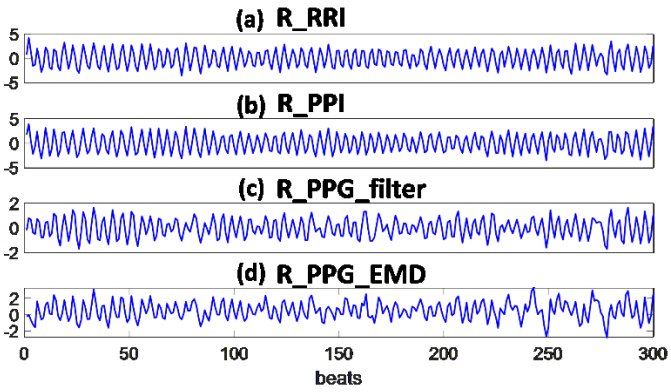

Fig. 4. Example of four respiration time series extracted as the points in the acquired breathing signal corresponding to the timing of ECG R peaks (R_RRI, panel (a)) and of PPG peaks (R_PPI, panel (b)), and as the samples of the respiration signal reconstructed using the filtering approach (R_PPG_filter, panel (c)) and the EMD algorithm (R_PPG_EMD, panel (d))) also corresponding to the timing of PPG minima peaks.

On the contrary, PSD values computed for the first two settings (R_RRI and R_PPI) are comparable between each other and expectedly slightly increase with controlled breathing, since all the respiratory variability is centred around the respiration peak (~0.33 Hz) and spectral leakage was observed to be negligible.

As regards Granger causality measures, our results suggest that their overall behaviour is characterized by a decrease when these values are computed using respiratory time series reconstructed from the PPG, especially with regard to the spectral measure (see values in Table I). Generally, in the presence of bigger databases, statistical analysis is performed to detect significant changes of the investigated measures between experimental conditions or settings.

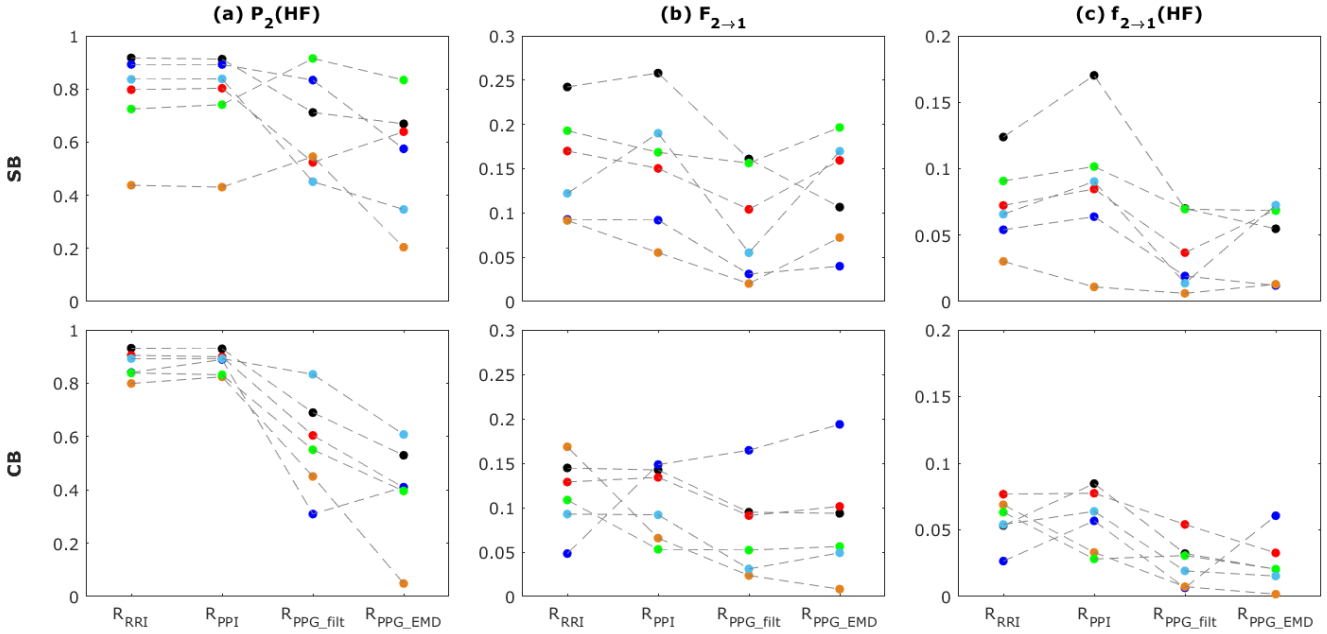

Fig. 5. Results of time domain and spectral analysis on the available time series H (process 1) and R (process 2). (a) Normalized power spectral density (PSD) of R in the HF band of the spectrum, computed as the ratio of the PSD in HF to the total PSD. (b) Time domain logarithmic Granger causality from the driver process (R) to the target (H), computed as the integral of (4) alongside the whole frequency spectrum. (c) Spectral measure of Granger causality from the driver process (R) to the target (H), computed as the integral of (4) within the HF band of the spectrum. Measures are computed in the two phases of the protocol (spontaneous breathing, SB, panels above; controlled breathing, CB, panels below) considering the four respiration time series described in section II.B (R_RRI, R_PPI, R_PPG_filter, R_PPG_EMD) for all 6 subjects (each subject is represented by a different color).

TABLE I
TIME AND FREQUENCY DOMAIN GRANGER CAUSALITY VALUES FOR EACH ANALYZED SUBJECT

	$F_{2\to1}$								$f_{2\to1}(HF)$							
	R_RRI		R_PPI		R_PPG_filter		R_PPG_EMD		R_RRI		R_PPI		R_PPG_filter		R_PPG_EMD	
	SB	CB	SB	CB	SB	CB	SB	CB	SB	CB	SB	CB	SB	CB	SB	CB
subject 1	0.24	0.14	0.26	0.14	0.16	0.09	0.11	0.09	0.12	0.05	0.17	0.08	0.07	0.03	0.05	0.02
subject 2	0.17	0.13	0.15	0.13	0.10	0.09	0.16	0.10	0.07	0.08	0.08	0.08	0.04	0.05	0.07	0.03
subject 3	0.09	0.05	0.09	0.15	0.03	0.16	0.04	0.19	0.05	0.03	0.06	0.06	0.02	0.01	0.01	0.06
subject 4	0.09	0.17	0.06	0.07	0.02	0.02	0.07	0.01	0.03	0.07	0.01	0.03	0.01	0.01	0.01	$<10^{-2}$
subject 5	0.19	0.11	0.17	0.05	0.16	0.05	0.20	0.06	0.09	0.06	0.10	0.03	0.07	0.03	0.07	0.02
subject 6	0.12	0.09	0.19	0.09	0.06	0.03	0.17	0.05	0.07	0.05	0.09	0.06	0.01	0.02	0.07	0.02

In previous works, this has allowed to characterize the possibly different behaviours of time domain measures and frequency-specific measures, which have been found to be more precise and informative than overall indices, especially when the observed processes exhibit frequency-specific oscillations [27], [28]. We could not perform statistical analysis because of the small number of samples employed, but this led to some difficulties in the interpretation of the obtained causality values in time and frequency domain. Several studies have documented that the magnitude of respiratory-related fluctuations of RRI (i.e., respiratory sinus arrhythmia) dramatically changes according to breathing rate [29]. Moreover, it has been demonstrated that paced breathing at ~0.25 Hz does not alter efferent vagal and sympathetic modulations in the frequency range from 0.04 Hz to 0.15 Hz in healthy subjects [8], [30]. In this study, we found a decrease of both time and spectral measures in CB with respect to SB in 3 subjects (50%), while increased or unchanged values were detected in the remaining samples (Table I). These findings must be further investigated according to the subject-specific spontaneous breathing rate and with bigger datasets. The possibility to enroll a larger number of subjects and carry out statistical analyses represents one of the future extensions of this study, that will enable a more clear assessment of the feasibility of the proposed approaches for the extraction of respiration from the PPG. Nonetheless, our preliminary findings suggest that causality measures behave similarly if the PPG is used in place of the ECG for the detection of heart period and the sampling of respiration. On the other hand, the filtering and EMD approaches for the extraction of respiration from the PPG may be less accurate in the quantification of time domain and spectral measures, and especially of respiratory PSD. Indeed, applying a PPG bandpass filter to identify respiratory dynamics may cause misdetection of power content if other oscillatory components are present within the selected HF range or if the peak bandwidth is too large. Conversely, the EMD extraction technique is based on how well the detection of PPG peaks is performed, and this may pose a problem when the acquired waveform is noisy, due e.g. to motion artifacts.

IV. CONCLUSION

In the present study, starting from the data acquired from our portable multisensor portable system, the feasibility of using the less invasive and more cost-efficient PPG technique in place of the standard ECG for investigating

cardiorespiratory interactions has been proved, since the computation of respiratory parameters and patterns of causality in time and spectral domain provided similar results when heart period is taken as the PPI sequence instead of RRI sequence. However, our findings also suggest that the use of PPG for the extraction of the respiration signal could lead to underestimates of the computed measures. This aspect should be further investigated and validated with wider databases and statistical analyses.

ACKNOWLEDGMENT

GV Ph.D. grant was supported by Istituto Nazionale Previdenza Sociale (INPS) Ph.D. fellowship, project title "Sviluppo di protocolli sperimentali e impiego di soluzioni tecnologiche finalizzate alla valutazione oggettiva e quantitativa dello stress lavoro-correlato". SV Ph.D. grant was supported by the Italian MIUR PON R&I 2014-2020 "Dottorati innovativi con caratterizzazione industriale" funding programme. RP was supported by the Italian MIUR PON R&I 2014-2020 AIM project no. AIM1851228-2. LF was supported by the Italian MIUR PRIN 2017 project 2017WZFTZP "Stochastic forecasting in complex systems". We kindly thank the support of PO PSN project no. 2017/4.1.14 and of Dr. Salviato and Dr. Carruba (ARNAS Ospedali Civico Di Cristina-Benfratelli, Palermo, Italy), and of Italian Ministry of Education, University and Research "Sensoristica intelligente, infrastrutture e modelli gestionali per la sicurezza di soggetti fragili" (4FRAILTY) project (PON R&I ARS01_00345).

REFERENCES

[1] A. Bashan, R. P. Bartsch, J. W. Kantelhardt, S. Havlin, and P. C. Ivanov, "Network physiology reveals relations between network topology and physiological function," *Nat. Commun.*, vol. 3, p. 702, Feb. 2012.

[2] R. Pernice *et al.*, "Multivariate Correlation Measures Reveal Structure and Strength of Brain–Body Physiological Networks at Rest and During Mental Stress," *Front. Neurosci.*, vol. 14, p. 1427, 2021.

[3] A. Stefanovska, "Cardiorespiratory interactions," vol. 1, no. 2001, pp. 462–469, 2002.

[4] I. Lazic, R. Pernice, T. Loncar-Turukalo, G. Mijatovic, and L. Faes, "Assessment of Cardiorespiratory Interactions during Apneic Events in Sleep via Fuzzy Kernel Measures of Information Dynamics," *Entropy*, vol. 23, no. 6, p. 698, 2021.

[5] M. Javorka *et al.*, "Respiratory Sinus Arrhythmia Mechanisms in Young Obese Subjects," *Front. Neurosci.*, vol. 14, p. 204, 2020.

[6] L. A. Lipsitz, J. Hayano, S. Sakata, A. Okada, and R. J. Morin, "Complex demodulation of cardiorespiratory dynamics preceding vasovagal syncope," *Circulation*, vol. 98, no. 10, pp. 977–983, 1998.

[7] D. L. Eckberg, "Point: counterpoint: respiratory sinus arrhythmia is due to a central mechanism vs. respiratory sinus arrhythmia is due to the baroreflex mechanism," *J. Appl. Physiol.*, 2009.

[8] G. D. Pinna, R. Maestri, M. T. La Rovere, E. Gobbi, and F. Fanfulla, "Effect of paced breathing on ventilatory and cardiovascular variability parameters during short-term investigations of autonomic function," *Am. J. Physiol. - Hear. Circ. Physiol.*, vol. 290, no. 1, pp. 424–433, 2006.

[9] R. Pernice *et al.*, "Reliability of Short-Term Heart Rate Variability Indexes Assessed through Photoplethysmography," in *2018 40th Annual International Conference of the IEEE Engineering in Medicine and Biology Society (EMBC)*, 2018, pp. 5610–5613.

[10] R. Pernice *et al.*, "Low invasive multisensor acquisition system for real-time monitoring of cardiovascular and respiratory parameters," *20th IEEE Mediterr. Electrotech. Conf. MELECON 2020 - Proc.*, pp. 306–310, 2020.

[11] R. Pernice, A. Parisi, G. Adamo, S. Guarino, L. Faes, and A. Busacca, "A portable system for multiple parameters monitoring: towards assessment of health conditions and stress level in the automotive field," in *2019 AEIT International Conference of Electrical and Electronic Technologies for Automotive (AEIT AUTOMOTIVE)*, 2019, pp. 1–6.

[12] C. W. J. Granger, "Investigating causal relations by econometric models and cross-spectral methods," *Econom. J. Econom. Soc.*, pp. 424–438, 1969.

[13] J. Geweke, "Measurement of linear dependence and feedback between multiple time series," *J. Am. Stat. Assoc.*, vol. 77, no. 378, pp. 304–313, 1982.

[14] G. Adamo *et al.*, "Signal to Noise Ratio of silicon photomultipliers measured in the continuous wave regime," in *2014 Third Mediterranean Photonics Conference*, 2014, pp. 1–3.

[15] J. Hohl and S. Rush, "The complete heart-lead relationship in the einthoven triangle," *Bull. Math. Biophys.*, vol. 30, no. 4, pp. 615–623, 1968.

[16] J. Pan and W. J. Tompkins, "A Real-Time QRS Detection Algorithm," *IEEE Trans. Biomed. Eng.*, vol. BME-32, no. 3, pp. 230–236, 1985.

[17] A. Fusco, D. Locatelli, F. Onorati, G. C. Durelli, and M. D. Santambrogio, "On how to extract breathing rate from PPG signal using wearable devices," in *2015 IEEE Biomedical Circuits and Systems Conference (BioCAS)*, 2015, pp. 1–4.

[18] F. Shaffer and J. P. Ginsberg, "An Overview of Heart Rate Variability Metrics and Norms," *Front. public Heal.*, vol. 5, p. 258, Sep. 2017.

[19] P. H. Charlton *et al.*, "Extraction of respiratory signals from the electrocardiogram and photoplethysmogram: technical and physiological determinants," *Physiol. Meas.*, vol. 38, no. 5, p. 669, 2017.

[20] K. V. Madhav, M. R. Ram, E. H. Krishna, N. R. Komalla, and K. A. Reddy, "Estimation of respiration rate from ECG, BP and PPG signals using empirical mode decomposition," in *2011 IEEE International Instrumentation and Measurement Technology Conference*, 2011, pp. 1–4.

[21] D. Nuzzi, L. Faes, M. Javorka, D. Marinazzo, and S. Stramaglia, "Inclusion of instantaneous influences in the spectral decomposition of causality: Application to the control mechanisms of heart rate variability," *Eur. Signal Process. Conf.*, vol. 2021-Janua, pp. 930–934, 2021.

[22] L. Faes, S. Erla, A. Porta, and G. Nollo, "A framework for assessing frequency domain causality in physiological time series with instantaneous effects," *Philos. Trans. R. Soc. A Math. Phys. Eng. Sci.*, vol. 371, no. 1997, p. 20110618, 2013.

[23] L. Faes, S. Stramaglia, and D. Marinazzo, "On the interpretability and computational reliability of frequency-domain Granger causality," *F1000Research*, vol. 6, 2017.

[24] H. Akaike, "A new look at the statistical model identification," *IEEE Trans. Automat. Contr.*, vol. 19, no. 6, pp. 716–723, 1974.

[25] D. Chicharro, "On the spectral formulation of Granger causality," *Biol. Cybern.*, vol. 105, no. 5–6, pp. 331–347, 2011.

[26] S. Strano *et al.*, "Respiratory sinus arrhythmia and cardiovascular neural regulation in athletes.," *Med. Sci. Sports Exerc.*, vol. 30, no. 2, pp. 215–219, 1998.

[27] L. Sparacino, R. Pernice, G. Nollo, and L. Faes, "Causal and Non-Causal Frequency Domain Assessment of Spontaneous Baroreflex Sensitivity after Myocardial Infarction," in *2020 11th Conference of the European Study Group on Cardiovascular Oscillations (ESGCO)*, 2020, pp. 1–2.

[28] R. Pernice, L. Sparacino, G. Nollo, S. Stivala, A. Busacca, and L. Faes, "Comparison of frequency domain measures based on spectral decomposition for spontaneous baroreflex sensitivity assessment after Acute Myocardial Infarction," *Biomed. Signal Process. Control*, vol. 68, p. 102680, 2021.

[29] J. P. Saul, R. D. Berger, P. Albrecht, S. P. Stein, M. H. Chen, and R. J. Cohen, "Transfer function analysis of the circulation: Unique insights into cardiovascular regulation," *Am. J. Physiol. - Hear. Circ. Physiol.*, vol. 261, no. 4 30-4, 1991.

[30] J. E. Sanderson *et al.*, "Impact of changes in respiratory frequency and posture on power spectral analysis of heart rate and systolic blood pressure variability in normal subjects and patients with heart failure," *Clin. Sci.*, vol. 91, no. 1, pp. 35–43, 1996.